Thermodynamic analysis of carbamate formation and carbon dioxide absorption in *N*-methylaminoethanol solution

Min Xiao, Wenchao Zheng, Helei Liu*, Xiao Luo, Hongxia Gao, Zhiwu Liang*

Joint International Center for CO_2 Capture and Storage (iCCS), Hunan Provincial Key Laboratory for Cost-effective Utilization of Fossil Fuel Aimed at Reducing CO_2 Emissions, College of Chemistry and Chemical Engineering, Hunan University, Changsha 410082, PR China

*Corresponding author: zwliang@hnu.edu.cn (Z. Liang) & lhl0925@hotmail.com (H. Liu)

Abstract

Protonation and carbamate formation are critical reactions for CO_2 capture using amine-based absorbents which impact both CO_2 absorption and amine regeneration. In this regard, thermodynamic analysis towards CO_2 absorption in *N*-methylaminoethanol solution is carried out with specific attention to the corresponding protonation and carbamate formation reactions. The CO_2 absorption mechanism is investigated with the acquisition of reaction equilibrium constant and heat of reaction. CO_2 absorption performance of *N*-methylaminoethanol solution was evaluated in terms of CO_2 loading and solution pH. A thermodynamic model was then developed to mathematically describe the investigated system and make prediction on equilibrium CO_2 solubility, species profiles, and absorption/regeneration heat. Results show that the average relative deviation of equilibrium CO_2 solubility calculated from the is 4.2%. The predictive species profile and CO_2 absorption heat of *N*-methylaminoethanol solution indicates less energy cost in amine regeneration. This is in line with the relative unstable *N*-methylaminoethanol carbamate formation and consequential conversion to (bi)carbonate. The position of *N*-methylaminoethanol as potential absorbent for carbon capture is shown in terms of chemical reaction constants, equilibrium CO_2 solubility, second order rate constant (k_2), and pKa.

Key words: CO_2 capture; amine absorbent; thermodynamic analysis; modeling; reaction heat; molecular structure.

1. Introduction

Evidence suggests that excessive CO_2 emissions are the primary cause of global climate change that in turn is thought to contribute to present-day extremes in weather [1]. Post-combustion carbon capture (PCC) using amine solution is one of the most mature technologies to reduce CO_2 emission from flue gas [2, 3]. The development of alternative suitable amine solvents for efficient CO_2 absorption and amine regeneration is ongoing since the common amines such as monoethaolamine (MEA), diethanolamine (DEA) and *N*-methyldiethanolamine (MDEA) suffer from conspicuous drawbacks to limit its industrial application [4]. For example, primary amine is limited by maximum CO_2 solubility while tertiary amine has low CO_2 absorption rate. There is requirement to replenish fresh amine regularly due to amine loss and degradation. And more important, the energy penalty for CO_2 loaded amine regeneration has great impact to energy consumption and carbon capture cost. Blend absorbent with different kinds of amine is hence proposed to take advantage of their individual properties such as fast absorption rate of primary amines and low regeneration energy cost of tertiary amines [5-7]. However, this may also lead to more complicated tuning issues including degradation and corrosion among others. Some absorbents with new carbon capture concept have been proposed in order to reduce energy consumption for regeneration. The idea of biphasic absorbent is phase split after CO_2 absorption to form one liquid phase with higer CO_2 loading and another liquid phase with less CO_2 in solution. Only rich CO_2 solution is sent to stripper for absorbent regeneration to drop heating energy requirement [8, 9]. Water-lean

absorbent is used to reduce water composition for its high heat capacity and latent heat [10]. However, the practical application of these new concept CO_2 absorbents in PCC also has challenges and needs more investigation before scaling up.

Plenty of researches have been done to reveal the relationship between chemical-physical properties and amine molecular structure for CO_2 capture [11, 12]. *N*-methylaminoethanol (MAE) is proved as a potential absorbent candidate with multiple advantages regarding CO_2 capture. First of all, high maximum CO_2 solubility is observed when using MAE solution to absorb CO_2 [13]. This may be explained by the carbamate hydrolysis at high CO_2 loading region which is then approved by Folgueira, Teijido, Garcia-Abuin, Gómez-Díaz and Rumbo through NMR spectroscopy [14]. The hydrolysis of MAE carbamate implies the regeneration of CO_2 loaded MAE solution can be easier and less energy consumption due to the consequential bicarbonate/carbonate formation. Mimura, Suda, Iwaki, Honda and Kumazawa showed that CO_2 absorption rate of MAE is comparable to that of the benchmark amine MEA, and higher than that of the secondary amines ethylaminoethanol (EAE) and butylaminoethanol (BAE) [15]. In addition, the crucial physical properties of MAE are very competitive with MEA such as low vapour pressure and viscosity, comparable boiling point and higher physical CO_2 solubility [16]. Therefore, MAE may provide an additional option of CO_2 absorbent as a trade-off between CO_2 absorption rate, loading capacity, energy cost and critical physical properties. Despite MAE shows such good potential in the application of CO_2 capture, the crucial carbamate formation reaction concerning the straight

interaction between MAE and CO_2 hasn't been studied. The carbamate formation accompany with protonation is significant to understand the CO_2 absorption behavior and the corresponding reaction constant is necessary for model development.

Kent and Eisenberg developed a classical thermodynamic model for acid gas absorption into amine solution [17]. This semi-empirical model adopted published equilibrium constants for the chemical reactions in the studied system and fitted dissociation and carbamate formation constants with the CO_2 loading data. Deshmukh and Mather proposed an activity coefficient model for predicting partial pressure of CO_2 over MEA aqueous solutions [18]. The Deshmukh-Mather model adopted the activity coefficient based on the extended Debye-Hückel theory for electrolyte solutions, which has been successfully applied for a few amines to make reasonable extrapolations. Benamor and Aroua analysed equilibrium CO_2 solubility and carbamate species concentration in DEA and its mixture with MDEA solution using Deshmukh-Mather model [19]. Goharrokhi, Taghikhani, Ghotbi and Safekordi used the extended Debye-Hückel model to study and make accurate prediction for MDEA-CO_2-H_2O system [20]. Afkhamipour and Mofarahi applied Deshmukh-Mather model to predict equilibrium CO_2 solubility data in 1-dimethylamino-2-propanol solution with average relative deviation of 2.64% [21]. Pakzad, Mofarahi, Izadpanah, Afkhamipour and Lee investigated 2-amino-2-methly-1-propanol + N-methyl-2-pyrrolidone system and correlated experimental data using Deshmukh-Mather model to calculate CO_2 loading, species concentration and CO_2 absorption heat [22].

This work studies chemical reactions that MAE participates during CO_2 absorption as well as phase behavior of MAE-CO_2-H_2O ternary system, aiming to bridge the knowledge gap between these two different scales. Specifically, the pH value of the acidified MAE solution is measured to obtain the dissociation reaction constant. The carbamate formation constant of MAE solution was measured through titration of MAE-$NaHCO_3$ solution. The enthalpies and entropies of the dissociation and carbamate formation constants were derived using the van 't Hoff equation. CO_2 absorption was carried out to measure CO_2 loading and pH of amine solutions versus time. A thermodynamic model was developed for the investigated system to predict equilibrium CO_2 solubility as a function of temperature, CO_2 partial pressure and initial amine concentration. The prediction results were found to agree well with the experimental data. Extrapolated predictions were made to give more CO_2 solubility information over a wider range of conditions. The species profile of MAE solution and CO_2 absorption heat were predicted based on the model data. Finally, MAE was compared with various amines in terms of chemical reaction constant, equilibrium CO_2 solubility, pKa and second order rate constant (k_2) to give a general evaluation of MAE as an absorbent for CO_2 capture.

2. Experimental section

2.1. Materials

Carbon dioxide (99%) was purchased from Changsha RIZHENG Gas Co., Ltd. Methylethanolamine (99%) and monoethanolamine (99%) were purchased from

Shanghai Macklin Biochemical Co., Ltd. Methyldiethanolamine (98%) and sodium hydroxide standard solution (1.000 M) was obtained from Aladdin Industrial Corporation. Sodium perchlorate monohydrate with purity of 99% was obtained from Shanghai Hushi Laboratorial Equipment Co., Ltd. All chemicals were used without further purification. Deionized water was used in the experiments for the preparation of solutions. The mass flow controller (D07) was purchased from Beijing Sevenstar Electronics Co., Ltd. A thermostatic water-circulator bath was purchased from HANUO, HX20 Shanghai Hannuo Instruments Co. Ltd. The pH meter with electrode model E-201-C with accuracy of ± 0.01 pH units was obtained from INESA Scientific Instruments Co., Ltd.

2.2. Measurement of dissociation and carbamate formation constant

A quantitative of amine was dissolved in deionized water to make 100 mL of 0.05 $mol \cdot L^{-1}$ solution. The solution was titrated using 1.0 $mol \cdot L^{-1}$ hydrochloric acid solution at 298, 303, 308, 313 and 318 K to measure the pH value. 0.5 mL HCl was introduced into the bulk solution stepwise and allowed to reach equilibrium prior to measurement. The total volume of HCl used was 5.0 mL. The dissociation constant of protonated MAE was calculated from the pH data. The volume increase of the bulk solution was taken into consideration in the calculation.

The measurement of the carbamate formation constant was similar to that in the work of Aroua, Armor and Haji-Sulaiman [23]. The amine solutions were prepared at concentration of 0.2 $mol \cdot L^{-1}$ with $NaHCO_3$ concentration of 0.5, 1.0 and 1.5 $mol \cdot L^{-1}$ respectively. For each MAE/$NaHCO_3$ ratio, a quantitative amount of $NaClO_4$ was

added with concentration of 0.0, 0.5, 1.0 and 1.5 mol·L^{-1} to adjust the ionic strength of the bulk solution. Temperature of the prepared solutions was maintained at 303, 313, 323 and 333 K using the water bath for twenty-four hours to reach equilibrium. The uncertainty of the temperature controller is ± 0.1 K. Then the solution was titrated with standard NaOH solution using a potentiometric titrator. The experiment was carried out three times as usual to guarantee reproducibility of the measurement.

2.3. CO_2 absorption

CO_2 absorption was carried out using a continuous flow reactor as shown in Figure 1. CO_2 absorption is briefly explained as follows: CO_2 gas from the cylinder passed through the mass flow meter (calibrated by soap film flow meter) with flow rate of 100 mL·min^{-1} in total. A water saturation cell was provided to balance the water loss. A reactor cell was immersed in a water bath at 298 K with a temperature controller. A total volume of 150 mL aqueous amine solution with concentration of 1.0 mol·L^{-1} was introduced into the reactor cell. Then, the gas was injected into the reactor cell after being saturated with water. A condenser was set on the top of reactor to reduce losses due to evaporation. The liquid sample was taken from bulk solutions to analyze CO_2 loading using Chittick apparatus at 5, 10, 15, 20, 30, 40, 60, 90 and 120 minutes. The pH value of the bulk solution was also measured. A detailed description of the titration technique could be found in our previous work [24].

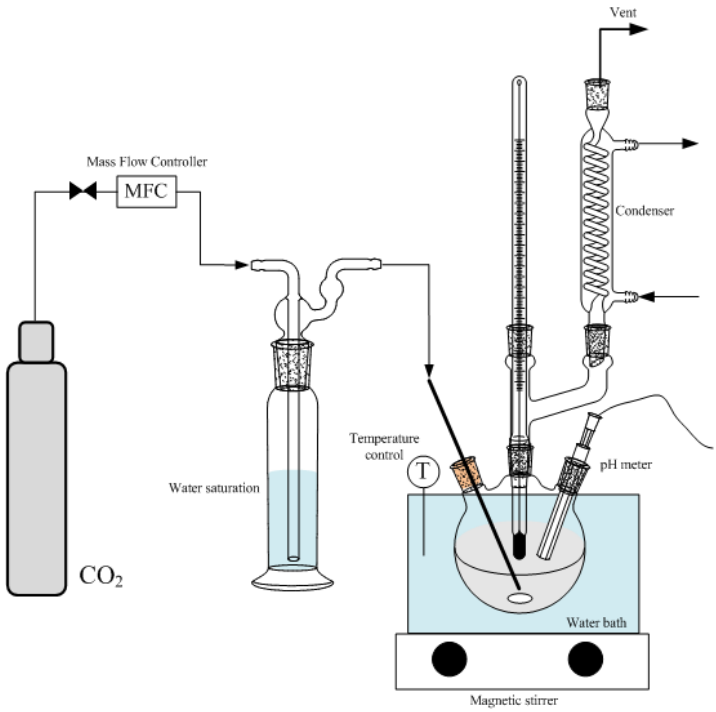

Figure 1. The schematic diagram of CO_2 absorption apparatus.

3. Theory

3.1. Reaction chemistry

The detailed description on thermodynamic model establishment has been shown in our previous work. The chemical reactions in the CO_2 absorption into MAE solution and the carbamate formation experiment are similar:

$$MAEH^+ \overset{K_1}{\leftrightarrow} MAE + H^+$$

$$MAE + HCO_3^- \overset{K_2}{\leftrightarrow} MAECOO^- + H_2O$$

$$CO_2 + H_2O \overset{K_3}{\leftrightarrow} HCO_3^- + H^+$$

$$H_2O \overset{K_4}{\leftrightarrow} H^+ + OH^-$$

$$HCO_3^- \overset{K_5}{\leftrightarrow} H^+ + CO_3^{2-}$$

The equilibrium constants of the reactions are given as:

$$K_1 = \frac{[MAE][H^+]}{[MAEH^+]}\frac{\gamma_{MAE}\gamma_{H^+}}{\gamma_{MAEH^+}} \quad (1)$$

$$K_2 = \frac{[MAECOO^-]}{[MAE][HCO_3^-]}\frac{\gamma_{MAECOO^-}}{\gamma_{[MAE]}\gamma_{HCO_3^-}} = K_2'\frac{\gamma_{MAECOO^-}}{\gamma_{[MAE]}\gamma_{HCO_3^-}} \quad (2)$$

$$K_3 = \frac{[HCO_3^-][H^+]}{[CO_2]}\frac{\gamma_{HCO_3^-}\gamma_{H^+}}{\gamma_{CO_2}} \quad (3)$$

$$K_4 = \frac{[H^+][OH^-]}{a_w}\gamma_{H^+}\gamma_{OH^-} \quad (4)$$

$$K_5 = \frac{[H^+][CO_3^{2-}]}{[HCO_3^-]}\frac{\gamma_{H^+}\gamma_{CO_3^{2-}}}{\gamma_{HCO_3^-}} \quad (5)$$

where $[i]$ and γ_i are the concentration and activity coefficient of species i respectively, K_i is the thermodynamic equilibrium constant, K_2' is the apparent equilibrium constant, and a_w is the water activity and equal to its mole fraction.

The activity coefficient can be expressed as:

$$\ln \gamma_i = -\frac{AZ_i^2\sqrt{I}}{1+B\sqrt{I}} + 2\sum \beta_{ij}[j] \quad (6)$$

where A is the Debye-Hückel constant; B is given as an empirical value of 1.2, Z_i represents charge on species i, I is ionic strength of solution, and β_{ij} refers to interaction parameter between species i and j.

The ionic strength of solution I can be written as:

$$I = \frac{1}{2}\sum [i]\, Z_i^2 \quad (7)$$

The binary interaction parameter is regarded as a linear function of temperature:

$$\beta_{ij} = a_{ij} + b_{ij}T \quad (8)$$

where a_{ij} and b_{ij} are correlated parameters.

3.2. Chemical speciation in the carbamate formation experiment

Besides the equations used to describe the equilibrium constants, some additional equations are given about mass balance and charge balance in bulk solution:

Amine balance:

$$[MAE] + [MAEH^+] + [MAECOO^-] = [MAE]_t \quad (9)$$

CO_2 balance:

$$[MAECOO^-] + [HCO_3^-] + [CO_3^{2-}] = \alpha \times [MAE]_t \quad (10)$$

Sodium balance:

$$[Na^+]_t = [NaHCO_3]_t + [NaClO_4]_t \quad (11)$$

Charge balance:

$$[MAEH^+] + [H^+] + [Na^+]_t = [HCO_3^-] + 2[CO_3^{2-}] + [OH^-] + [MAECOO^-] + [ClO_4^-]_t \quad (12)$$

where $[i]_t$ is referred to the initial concentration of the species *i*. When the equilibrium MAE-H_2O-$NaHCO_3$-$NaClO_4$ system is titrated with NaOH standard solution, only the bicarbonate and protonated amine will be consumed, which gives an equation:

$$B = [MAEH^+] + [HCO_3^-] \quad (13)$$

where *B* is the concentration of NaOH at the end point.

3.3. Chemical speciation in the CO_2 absorption experiment

Although the chemistry in the CO_2 absorption experiment is similar to that in the carbamate formation experiment, the equations of CO_2 and charge balance vary due to lack of species Na^+ and ClO_4^-:

CO_2 balance:

$$[MAECOO^-] + [HCO_3^-] + [CO_3^{2-}] + [CO_2] = \alpha \times [MAE]_t \quad (14)$$

Charge balance:

$$[MAEH^+] + [H^+] = [HCO_3^-] + 2[CO_3^{2-}] + [OH^-] + [MAECOO^-] \quad (15)$$

where $[MAE]_t$ is initial concentration of MAE and α represents CO_2 solubility. The physical CO_2 solubility is small in bulk solution but still introduced in carbon balance to calculate CO_2 partial pressure according to Henry's law:

$$P_{CO_2} \times \emptyset_{CO_2} = He \times [CO_2] \times \gamma_{CO_2} \quad (16)$$

where P_{CO_2} is CO_2 partial pressure, $\emptyset_{CO_2}$ is CO_2 fugacity coefficient, and He is Henry's law constant for CO_2.

4. Results and discussion

4.1. Reaction constants of MAE solution

Protonation and carbamate formation are the major reactions that MAE participates in during CO_2 absorption. Acquiring of the equilibrium constants of the protonation and carbamate formation reactions is crucial to understanding the performance of MAE in CO_2 absorption. The dissociation constant, (dissociation is the reverse reaction of protonation) can be measured via acid-base titration. In this case, the dilute MAE solution was titrated using HCl solution to determine the pH value. The transformed dissociation constant p*Ka* can be calculated using Equation 17.

$$pKa = pH - \log\left(\frac{[MAE]}{[MAEH^+]}\right) - \log\left(\frac{\gamma_{MAE}}{\gamma_{MAEH^+}}\right) \quad (17)$$

It is noted that the second term $2\sum \beta_{ij}[j]$ in the activity coefficient (Equation 6) representing short-range Van der Waals forces is insignificant and can be neglected in the calculation of the dissociation and carbamate formation constants. The calculated results of p*Ka* are plotted in Figure 2 and show good agreement with the work of Littel, Bos and Knoop [25].

With the measured dissociation constant and constants K_3, K_4, K_5 and A extracted from the references as tabulated in Table 1 [26, 27], the concentration of all species in the equilibrium MAE-H_2O-$NaHCO_3$-$NaClO_4$ system can be calculated through solving Equations 1-7 and 9-13 simultaneously. The apparent equilibrium constant K_2' of Equation 2 is then obtained under various conditions e.g. temperature and ionic strength. It is noted that according to equation 2, K_2 is equal to the apparent equilibrium constant K_2' when ionic strength is zero. Therefore, $\log(K_2')$ is summarized in Figure 3 against $I^{0.5}$ to display a linear relationship where the intercept of the fitting curve at zero ionic strength is deemed the same value as $\log(K_2)$. The carbamate formation constants are tabulated in Table 2 as a function of temperature. The constants of dissociation (equation 1) and carbamate formation (equation 2) were then correlated using the van 't Hoff equation to quantify the standard-state molar enthalpies (ΔH_m^0) and entropies (ΔS_m^0):

$$\ln K = -\frac{\Delta H^0}{RT} + \frac{\Delta S^0}{R} \qquad (18)$$

The correlation results are summarized in Table 3 together with those of MEA, DEA and MDEA [23, 28-30]. It can be found that both dissociation and carbamate formation are enthalpy driven process as the much larger contribution of ΔH_m^0. A positive value of enthalpy indicates that the dissociation reaction is endothermic while a negative value suggests an exothermic process for the carbamate formation. Since the CO_2 absorption is combined with carbamate formation and protonation of the amine (the reverse process of dissociation), heat release is expected from the reaction during CO_2 absorption. More importantly, a large amount of energy is required to shift

the reaction to the proper side to regenerate the amine in CO_2 desorption.

In dissociation, the enthalpy of MAE (48.51 $kJ \cdot mol^{-1}$) is similar to that of MEA (48.05 $kJ \cdot mol^{-1}$) due to the similar molecular structure. DEA (42.87 $kJ \cdot mol^{-1}$) and MDEA (34.92 $kJ \cdot mol^{-1}$) show relatively lower enthalpy in dissociation as there are two additional hydroxyethyl groups in these molecules, reducing the activity of the nitrogen atom. It is noted that the absolute value of enthalpies of dissociation reactions are commonly larger than those of carbamate decompositions (the reverse reaction of carbamate formation). This indicates the dissociation reactions are more sensitive to any change in temperature. The dissociation entropy of MAE is similar to that of DEA and falls within typical range for secondary amine, which is normally lower than that of primary amine e.g. MEA and higher than that of tertiary amine e.g. MDEA [31].

The enthalpies of carbamate formation can be ranked as MEA < MAE < DEA to imply the carbamate in MEA solution is most stable and least sensitive to temperature while that in MAE and DEA solution is easier to decompose at high temperature. The substitute methyl or hydroxyethyl group linked to the nitrogen atom will create steric hindrance that serves to destabilize the formed carbamate. The entropy of MAE and DEA is comparable and lower than that of MEA, which also suggests the similar steric hindrance effect between the two secondary amines.

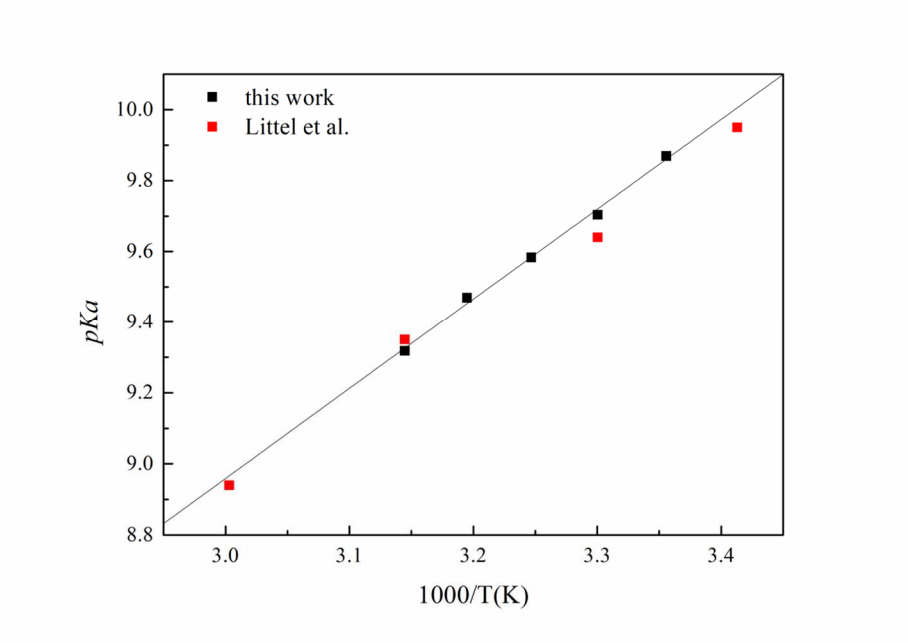

Figure 2. Comparison of MAE p*Ka* between experimental and literature value versus different temperature

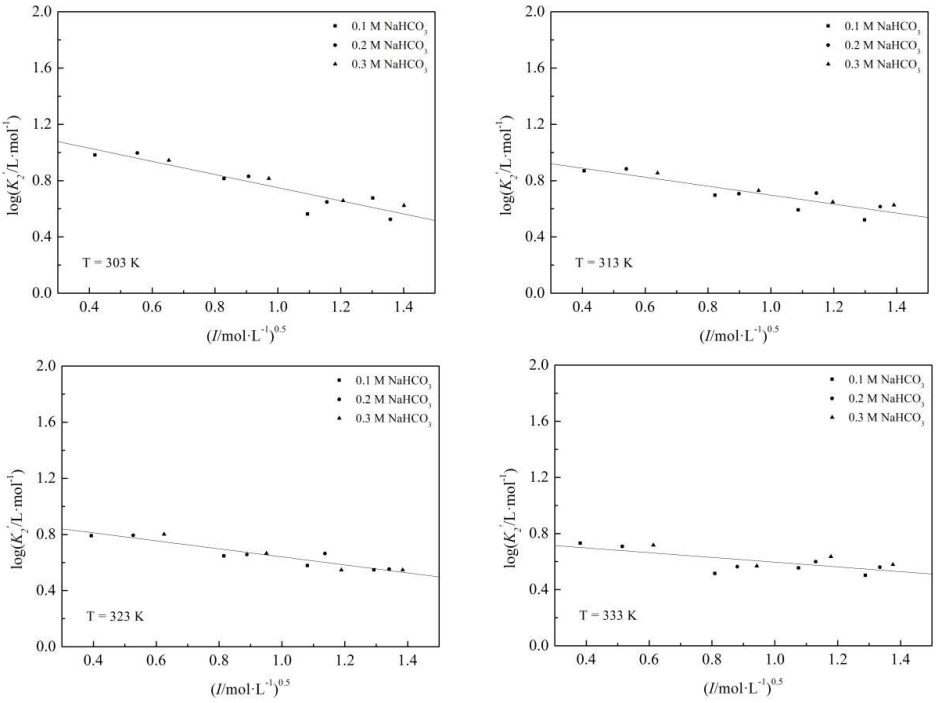

Figure 3. Equilibrium constants of carbamate formation (log(K_2)) versus ionic strength (I) under 303, 313, 323 and 333 K

Table 1. Constant expressions of K_n, He and A

Constant expressions	Source
$K_3 = \exp(235.482 - \frac{12092.1}{T} - 36.782 \ln T)$	[26]
$K_4 = \exp(140.932 - \frac{13445.9}{T} - 22.477 \ln T)$	[26]
$K_5 = \exp(220.067 - \frac{12431.7}{T} - 35.482 \ln T)$	[26]
$A = -1.307 + (1.328\text{E} - 2)T - (3.551\text{E} - 5)T^2 + (3.382\text{E} - 8)T^3$	[27]

Table 2. Equilibrium reaction constant for the carbamate formation of MAE

T/K	K_2/L·mol^{-1}
303	16.49
313	10.37
323	8.44
333	5.82

Table 3. Thermodynamic properties for the reactions

Reaction	Amine	ΔH_m^0/kJ·mol^{-1}	ΔS_m^0/kJ·K^{-1}·mol^{-1}	Source
Dissociation	MAE	48.51	-0.03	this work
	MEA	48.05	-0.02	[30]
	DEA	42.87	-0.03	[23, 29]
	MDEA	34.92	-0.05	[30]
Carbamate foramtion	MAE	-27.98	-0.07	this work
	MEA	-12.87	-0.02	[28]
	DEA	-33.85	-0.10	[23]
	MDEA	N/A	N/A	

4.2. CO_2 absorption

The absorption of CO_2 using MAE solution was studied to compare with the primary amine, MEA, and the tertiary amine, MDEA. The results are summarized in Figure 4 to show the CO_2 loading and pH value of the solution. As expected, the pH value decreases with increasing CO_2 loading. The initial CO_2 absorption rate within the first 15 minutes can be ranked as MAE (0.033 mol CO_2·mol amine^{-1} min^{-1}) ≈

MEA (0.031 mol CO_2·mol amine^{-1} min^{-1}) > MDEA (0.021 mol CO_2·mol amine^{-1} min^{-1}). MEA and MAE solutions approached maximum CO_2 loading at around 60 minutes. On the contrary, it takes about more than 120 minutes for the tertiary amine solutions to approach maximum CO_2 loading. There is no significant difference of initial CO_2 absorption rate between MAE and MEA solution, both of which are much faster than that of MDEA solution. The formation of carbamate in MAE solution provides an acceptable reaction rate in CO_2 absorption. In addition, the final CO_2 loading of MAE solution at 0.828 mol CO_2·mol amine^{-1} is higher than that of MDEA and MEA solution at 0.809 and 0.743 mol CO_2·mol amine^{-1} respectively at the given condition. This is due to fact that the conversion from carbamate to bicarbonate is favored by the stoichiometry and results in a higher molecular efficiency in CO_2 absorption. To conclude, MAE solution shows the highest CO_2 absorption efficiency among the three amines studied here in view of both absorption rate and CO_2 loading.

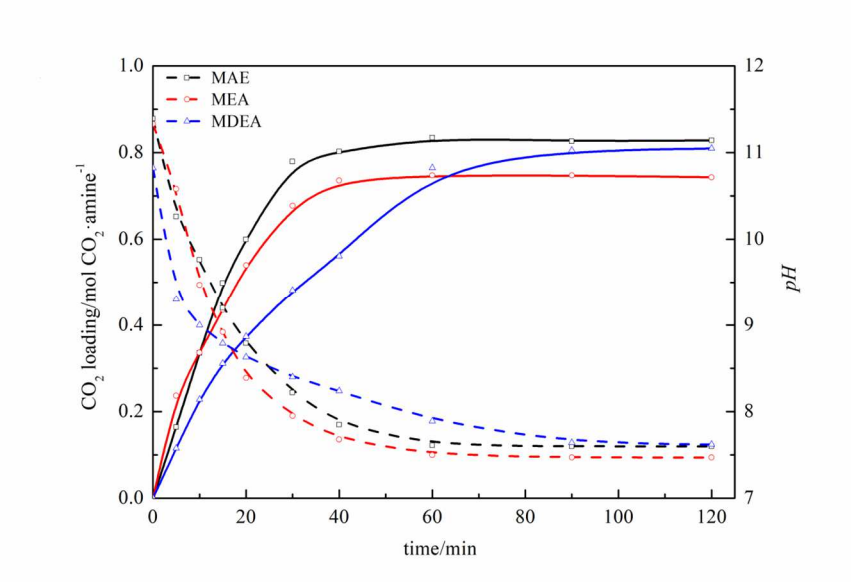

Figure 4. CO_2 absorption curves where solid curves are CO_2 loading and dashed curves are pH values

4.3. Thermodynamic modeling of MAE-CO_2-H_2O system

The capability of a thermodynamic model to correlate and predict vapour-liquid equilibrium data is vital in process design and simulation. A model should also be able to provide detailed information of species in the bulk solution to help understand the CO_2 absorption mechanism.

A thermodynamic model of the MAE-CO_2-H_2O system is established here based on the knowledge of the reaction equilibrium and phase equilibrium. The activity coefficient model applying six pairs of parameters to correlate the interactions between high concentration species MAE, $MAEH^+$, $MAECOO^-$, and HCO_3^- is introduced. For those species with low concentration e.g. CO_3^{2-}, $H^+$and OH^-, the second term of Equation 6 is ignored as little contribution was made. Note that the interaction with CO_2 was also considered due to the high pressure condition. CO_2 fugacity can be calculated using the Peng-Robinson equation of state [32].

The Henry's law constant of physical CO_2 solubility in aqueous MAE solution was derived from the N_2O solubility data from Luo, Su, Gao, Wu, Idem and Tontiwachwuthikul *et al* via their work with the 'N_2O analogy' [16]. The data was correlated with an exponential function and the fitting parameters are as tabulated in Table 4. The equilibrium CO_2 solubility data extracted from work of Haider, Yusoff and Aroua and Kumar and Kundu covered temperatures from 303 to 333 K, amine concentrations from 1.0 to 4.0 mol·L^{-1} and CO_2 partial pressures from 0.1 to 510 kPa [13, 33, 34]. It is pointed out that the model description is only validated within the given condition ranges and the extension to lean CO_2 loading region lower than 0.3

mol CO_2·mol amine^{-1} and high temperature up to 393 K for amine regeneration is limited. With the combination of Equations 1-9 and 14-16, the interaction parameters were optimized as shown in Table 5. The objective function of optimization is expressed as:

$$\mathrm{OF} = \sum \left| \frac{\alpha_{exp} - \alpha_{cal}}{\alpha_{exp}} \right| \qquad (19)$$

where α_{exp} is experimental equilibrium CO_2 solubility and α_{cal} represents calculated equilibrium CO_2 solubility.

Using the obtained interaction parameters, the final prediction results of equilibrium CO_2 solubility were compared with the experimental data to generate a parity plot as shown in Figure 5. In general, a good agreement was shown at given conditions with an average deviation of 4.2 %. The capability to make prediction under new conditions is shown in Figure 6 under temperatures from 293 to 333 K, CO_2 partial pressures from 0.003 to 1000 kPa and initial amine concentrations of 1.0 and 3.0 mol·L^{-1}. The temperature, CO_2 partial pressure and initial amine concentration have the most significant influence on the equilibrium CO_2 solubility. A higher temperature leads to lower equilibrium CO_2 solubility since the CO_2 absorption using amine solution is exothermic. CO_2 partial pressure has a positive effect on the equilibrium CO_2 solubility as a higher CO_2 partial pressure increases the effective CO_2 concentration in the liquid phase for the correlated chemical reaction. In addition, a higher amine concentration, which means more reactive component, is beneficial for absorbing more CO_2 as well. However, the increase of amine concentration will decrease CO_2/amine molar ratio based on Le Chatelier's principle,

resulting in a lower equilibrium CO_2 solubility.

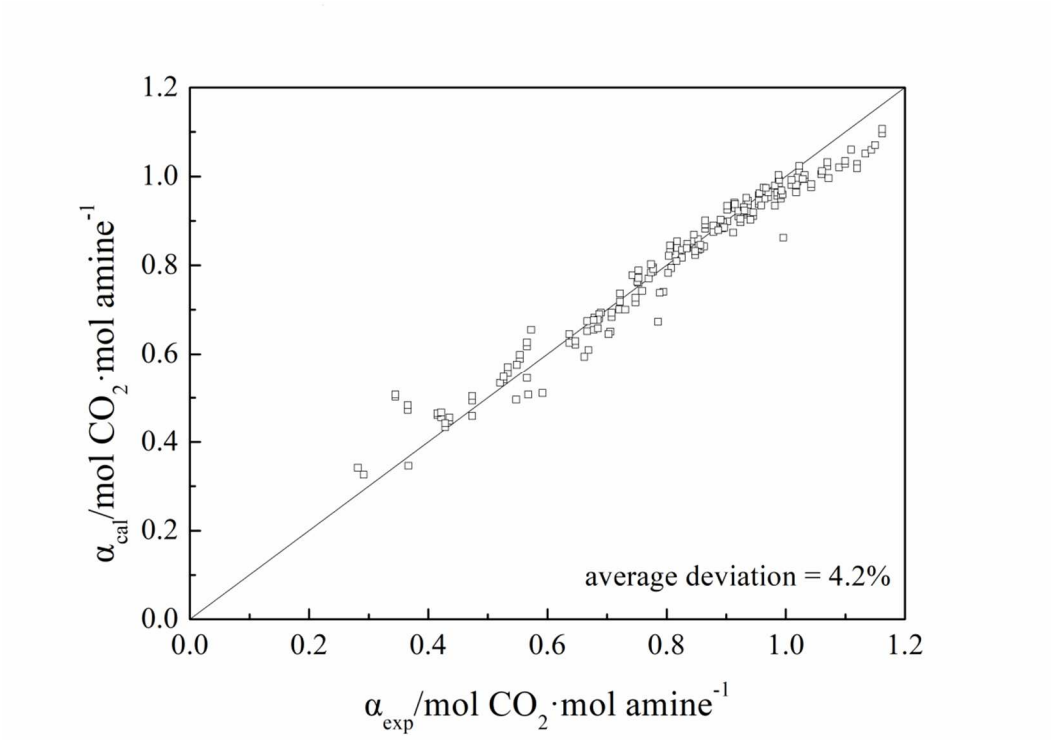

Figure 5. Parity plot of calculated equilibrium CO_2 solubility *vs* experimental data

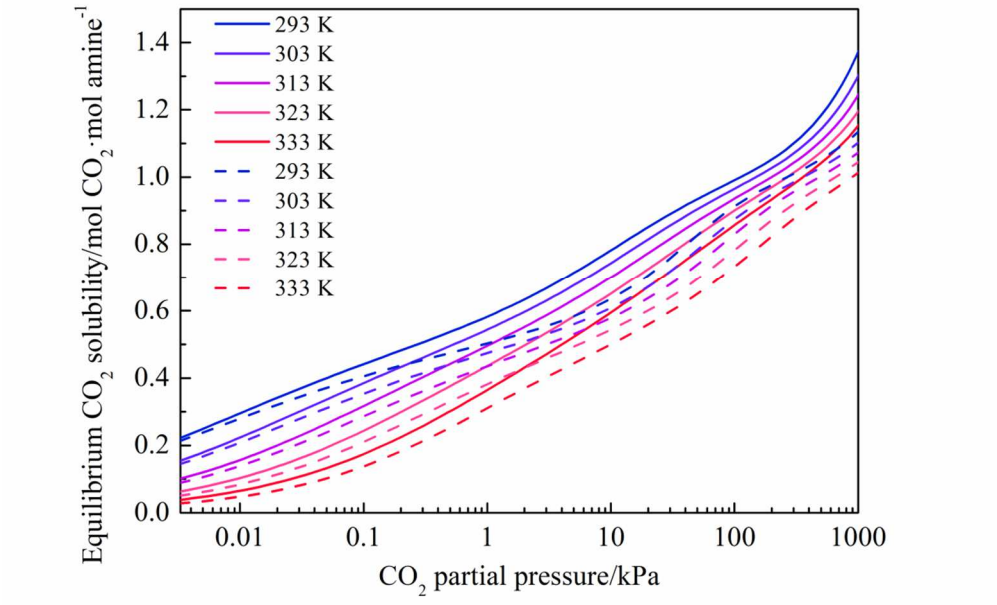

Figure 6. Prediction of equilibrium solubility, solid lines: 1.0 M; dashed lines: 3.0 M

Table 4. Henry's law constant ($Pa \cdot m^{-3} \cdot mol^{-1}$) of CO_2 in aqueous MAE solution[a]

$$He = \exp(B_1 + {}^{B_2}/_{T})$$

	b_0	b_1	b_2	b_3	b_4
B_1	-3.362E+02	-2.551E+03	1.458E+03	-3.218E+02	2.450E+01
B_2	8.787E+00	9.247E+00	-5.307E+00	1.183E+00	-9.101E-02

[a] the parameter was correlated using a polynomial equation of:

$$B = b_0 + b_1[MAE]_t + b_2[MAE]_t^2 + b_3[MAE]_t^3 + b_4[MAE]_t^4$$

Table 5. Binary interaction parameters β_{ij} for MAE-H_2O-CO_2 system

Species interaction	a_{ij}($L \cdot mol^{-1}$)	b_{ij}(L $K \cdot mol^{-1}$)
MAE- $MAEH^+$	-5.905E-01	1.817E-03
MAE - HCO_3^-	3.839E-01	-7.999E-04
MAE - $MAECOO^-$	-9.370E-01	3.280E-03
$MAEH^+$ - HCO_3^-	-2.635E-01	6.500E-04
$MAEH^+$ - $MAECOO^-$	-9.900E-01	3.548E-03
HCO_3^- - $MAECOO^-$	8.852E-01	-2.636E-03
CO_2- $MAEH^+$	1.525E-01	-2.548E-04
CO_2- HCO_3^-	-3.890E-01	8.861E-04

4.4. Speciation of MAE solution during CO_2 absorption.

The model was extended to calculate species profiles in the liquid phase of MAE to help understand the reaction process of CO_2 absorption into the amine solution. In the calculation, the restriction of phase equilibrium was removed by setting CO_2 partial pressure to be an unknown parameter. To validate the calculation result, the prediction was made at the temperature of 298 K with 1.0 M MAE solution. The corresponding solution pH values at different CO_2 solubility were obtained and compared with

experimental values. The comparison results are tabulated in Table 6 to show that the prediction result is reasonable with average deviation of 2.5% despite slight overprediction exists at CO_2 solubility of 0.828 mol CO_2·mol amine^{-1}. This overprediction may be due to the limited data at this region to correlate model. The deviation can be reduced by introducing more solubility data or additional species concentration information. The species profile of 1.0 mol·L^{-1} MAE solution at 298, 313 and 333 K is displayed in Figure 7 versus CO_2 loading from zero to 1.2 mol CO_2·mol amine^{-1}. With the increase of CO_2 loading:

- Free MAE is continuously consumed and the concentration of protonated MAE shows a steady increase while that of MAE carbamate drops after reaching maximum value of 0.34 mol·L^{-1} at 0.5 mol CO_2·mol amine^{-1} CO_2 loading
- Bicarbonate formation starts to contribute CO_2 absorption after loading higher than 0.2 mol CO_2·mol amine^{-1} and dominates the absorption process within CO_2 loading range between 0.5 to 0.9 mol CO_2·mol amine^{-1}.
- Carbonate makes a little contribution in CO_2 absorption but exhibits as a conjugated component of bicarbonate.
- The physical CO_2 concentration increases dramatically after CO_2 loading higher than 0.9 mol CO_2·mol amine^{-1}, indicating the major driving force changes from chemical absorption to physical absorption.
- A more rapid drop of hydroxide concentration is observed when CO_2 loading is lower than 0.2 mol CO_2·mol amine^{-1} and the drop slows down at higher loading. The concentration of proton is much lower in comparison with that of hydroxide.

Higher temperature leads to more bicarbonate and less MAE carbamate at same CO_2 loading but the concentration of protonated MAE is similar according to balance equation.

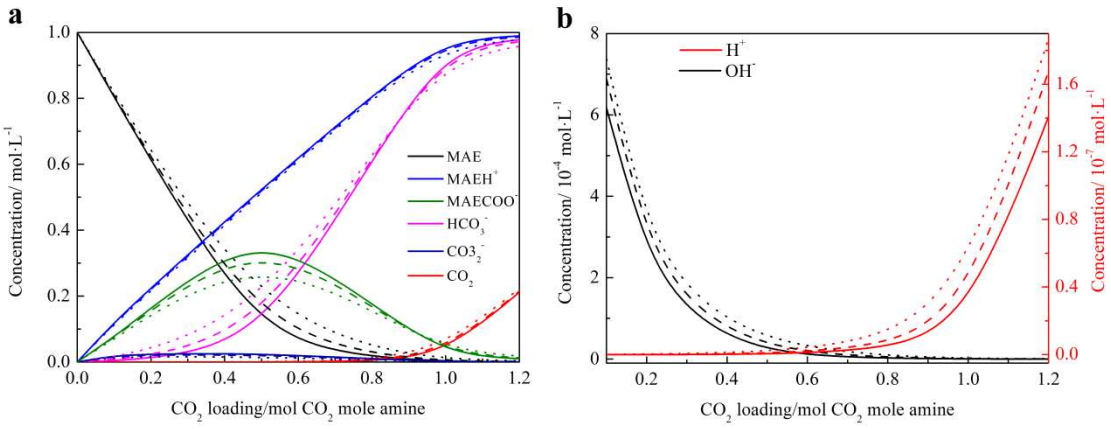

Figure 7. Calculated species profiles of CO_2 absorption with 1.0 mol·L^{-1} MAE solution. Solid lines: 298 K; Dashed lines: 313 K; Doted lines: 333 K.

Table 6. Experimental and calculated pH values of CO_2 loaded MAE solution at initial concentration of 1.0 mol·L^{-1} and temperature of 298 K

CO_2 solubility/mol CO_2·mol amine^{-1}	Experimental pH values	Calculated pH values	deviation
0.164	10.26	10.44	1.8%
0.335	9.76	9.87	1.1%
0.498	9.20	9.29	0.9%
0.600	8.79	8.92	1.5%
0.779	8.22	8.36	1.7%
0.828	7.60	8.20	7.9%

4.5. CO_2 absorption and desorption heat

Energy consumption in the regeneration of rich amine solution constitutes about 70-80% of the operation cost of the CO_2 capture process [35-37]. Developing amine solutions with lower CO_2 desorption heat is essential for further application of PCC

technology. Generally, the heat requirement to regenerate rich amine solution is provided through the reboiler whose duty can be approximated as the sum of three different terms as shown in Equation 20 [38]:

$$Q_{reb} = n_{CO_2}\Delta H_{des} + Q_{sen} + Q_{vap} \qquad (20)$$

where Q_{reb} is the reboiler duty; n_{CO_2} is the CO_2 stripping molar flow rate; ΔH_{Des} is the heat of CO_2 desorption to release CO_2 from amine solution; Q_{sen} is the sensible heat that used for the solvent in reboiler; Q_{vap} is the vaporization heat of water.

Since the vaporization heat of water is quite similar for aqueous amine solutions and the sensible heat is relatively small in comparison with other terms, the CO_2 desorption heat is dependent on the amine concentration and CO_2 loading which dominate the variations of reboiler duty in different amine systems [39]. It is reasonable to use CO_2 desorption heat as an indicator of reboiler energy consumption. The CO_2 desorption heat has the same absolute value as absorption heat since CO_2 desorption is a reverse process of CO_2 absorption. The absorption heat of MAE solution can be predicted using following simplified equation:

$$\frac{\partial}{\partial\left({}^{1}/_{\mathrm{T}}\right)}\left(\ln \mathrm{P}_{\mathrm{CO_2}}\right)_{\mathrm{p,n}} = \frac{-\Delta \mathrm{H}_{\mathrm{abs}}}{\mathrm{R}} \qquad (21)$$

where ΔH_{abs} represents the differential CO_2 absorption heat ($kJ \cdot mol^{-1}$), and R is the universal gas constant.

Svendsen, Hessen and Mejdell showed that the calculated desorption heat ΔH_{des} is quite sensitive to the original solubility data and the fitting procedure [40]. The correlation method as second order curve or linear curve may lead to significant

variation of ΔH_{des}. Thus, a narrow range of temperatures is preferred in this equation. This work applied calculated solubility data at 298, 303, 308 and 313 K as shown in Figure 8 to reduce the influence of the fitting procedure. In Figure 8, the slopes of linear fitting from $\ln P_{CO_2}$ against 1/T were extracted at different CO_2 loading as the term $\frac{-\Delta H_{abs}}{R}$ in the equation 21. The CO_2 absorption heat can therefore be calculated. For the fair comparison with 30 wt% MEA and MDEA, the differential CO_2 absorption heat of 30 wt% MAE (~ 4 mol·L^{-1}) solutions is calculated and displayed in Figure 9 [41-43]. No temperature dependency of CO_2 absorption heat is available in the application of equation 20. It is shown that the value is higher than that of MEA solution when CO_2 loading is lower than 0.3 mol CO_2·mol $amine^{-1}$. The CO_2 absorption heat curve of the 30 wt% MAE solution exhibits rapid decrease in advance of the 30 wt% MEA solution, indicating a premature carbamate decomposition, which is in consistent with the previous carbamate stability study. The lower CO_2 absorption heat indicates that the energy demand to regenerate rich MAE solution is lower than that of MEA solution. On the other hand, 30 wt% MDEA solution maintains relatively lower CO_2 absorption heat and no significant change of curve is observed due to the absorption mechanism.

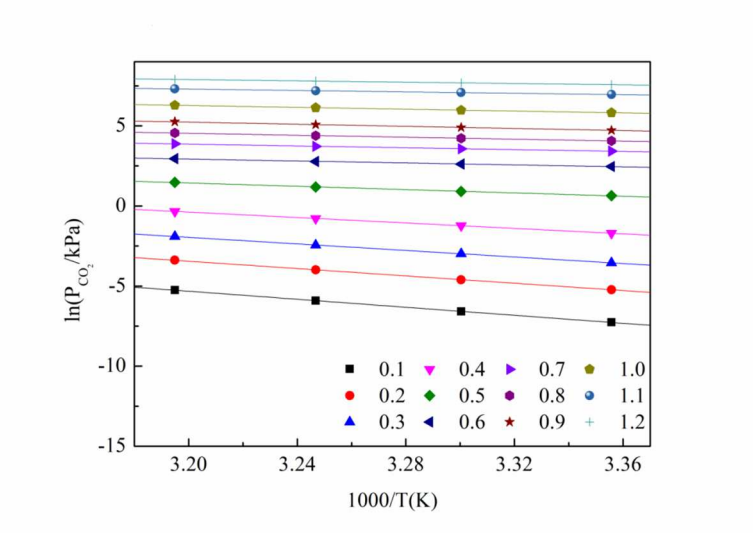

Figure 8. Linear fitting plot of $\ln P_{CO_2}$ against 1/T where legends are referred to CO_2 loading in mol CO_2·mol amine^{-1}.

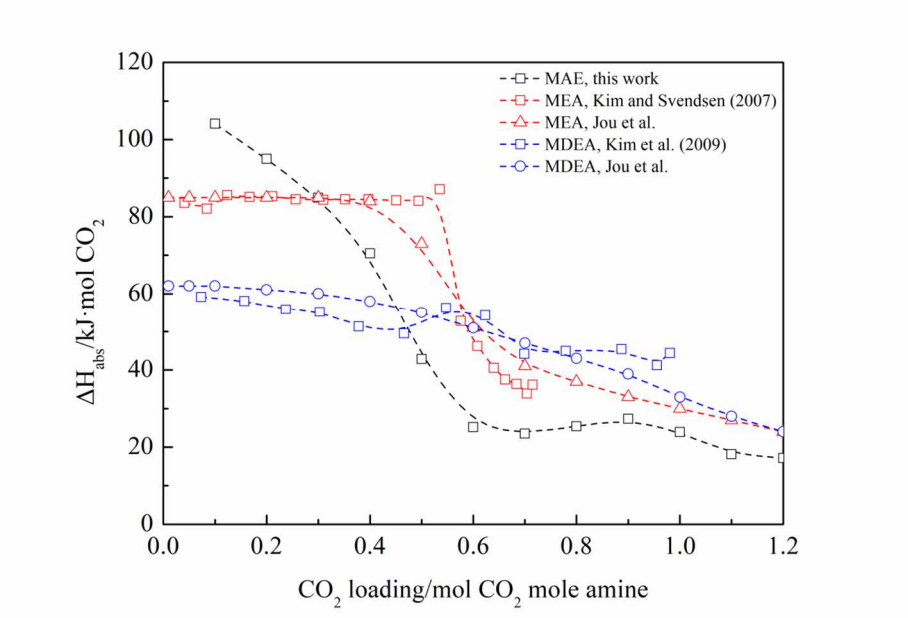

Figure 9. Differential CO_2 absorption heat ΔH_{abs} of 30 wt% MAE, MEA and MDEA solutions where MAE data were calculated using solubility data from 298 to 313 K.

4.6. General evaluation on MAE position for CO_2 capture

The comprehensive performance of MAE is evaluated to determine its potential for the formulation of good absorbents for CO_2 capture. The comparison is done with

benchmark amine MEA and other amines such as DEA and MDEA in view of chemical reactions with CO_2 and their various properties.

The protonated amine that balances the electro charge of the carbamate, bicarbonate and carbonate products is deemed a key component in amine solutions that absorb CO_2. The protonation behavior of amine is dependent on the electron density of the nitrogen atom and shows strong correlation to its molecular structure. The equilibrium constants of Equation 1 for the dissociation reaction are plotted in Figure 10 to show the rank order of: MAE < MEA < DEA < MDEA within a given temperature. In this figure, the amines DEA and MDEA with two hydroxyethyl groups have larger dissociation constants to show a lower ability to be protonated than MAE and MEA. MAE shows a lower dissociation constant than MEA because of an additional electron donating group linked to its nitrogen atom. The nature of easier protonation is beneficial for the promotion of hydrolysis of the acid gas.

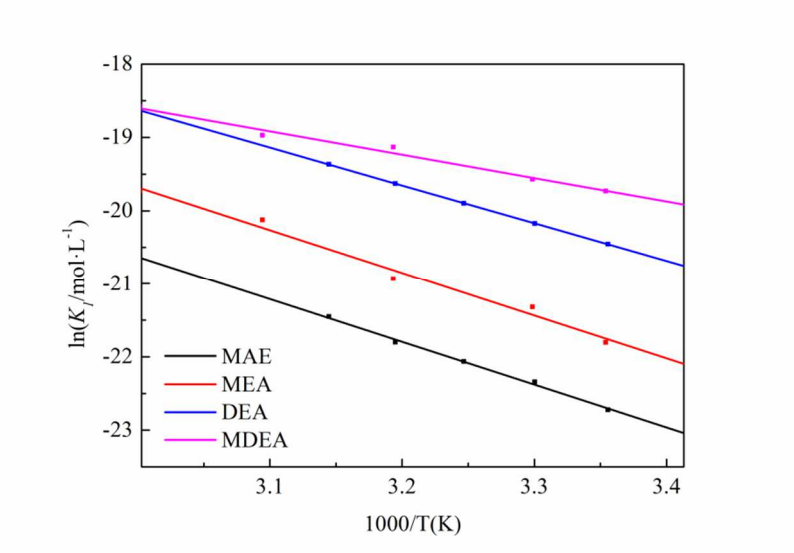

Figure 10. Equilibrium constant of dissociation as a function of temperature.

The equilibrium constants of Equation 2 for carbamate formation are summarized in Figure 11 to give an order of: MEA < MAE < DEA. There is no carbamate formation in tertiary amine solution when reacting with CO_2 thus MDEA is not included in this figure. It is found that attaching an additional substitute group on the nitrogen atom can effectively reduce the stability of the carbamate and the reduction is more obvious with the presence of a hydroxyethyl group instead of a methyl group. However, the hydroxylethyl group may also reduce the activity of the functional group and result in a poorer performance in CO_2 capture. In any case, the lower carbamate formation constant suggests an easier decomposition of MAE-carbamate. The conversion of carbamate to bicarbonate can lead to a lower CO_2 absorption heat as shown in Figure 9. A lower energy cost to regenerate rich amine solution is expected when MAE is applied in CO_2 capture. However, this is a premature evaluation and experimental desorption tests are required to justify that MAE has superior regeneration performance.

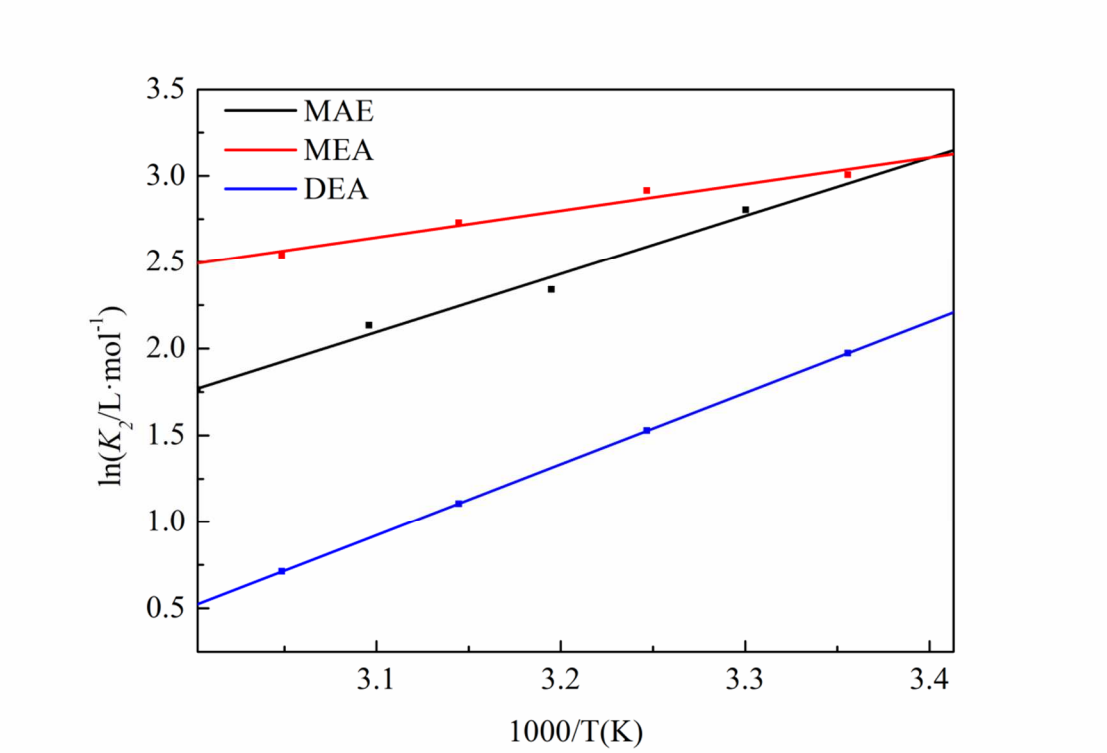

Figure 11. Equilibrium constant of carbamate formation as a function of temperature where points are experimental data and curves are fitting results.

In Figure 12, the equilibrium CO_2 solubility of MAE is further compared with MEA, 2-amino-2-methyl-1-propanol (AMP), DEA, MDEA and some tertiary amines, 1-dimethylamino-2-propanol (1DMA2P), 1-diethylamino-2-propanol (1DEA2P) and 4-diethylamino-2-butanol (DEAB) at initial amine concentration of 2.0 mol·L^{-1} and temperature of 313 K [24, 44]. The MAE solution data is as predicted in this work and other data are extracted from references [19, 45-48]. It shows that the equilibrium CO_2 solubility of MAE solution is at the middle stage of those amines. The methyl group linked to the nitrogen atom in the MAE molecule results in a favorable adjustment to the equilibrium CO_2 solubility in comparison with the primary (MEA) and secondary (DEA) amines. The solubility parameter is even comparable with the

outstanding tertiary amines which have high equilibrium CO_2 solubility. It is noted that although AMP is a primary amine, its stronger steric hindrance leads to a higher equilibrium CO_2 solubility. However, the kinetic behavior of the reaction between amine and CO_2 will also be affected by the strong steric hindrance.

An overall consideration of reaction rate, reaction kinetics and stoichiometric efficiency is required in order to accurately assess performance. In Figure 13, the second order reaction rate constant (k_2) and pKa of various primary, secondary and tertiary amines are extracted from the references for comparison. Those amines include MEA, AMP, MAE, DEA, MDEA, triethanolamine (TEA), dimethylethanolamine (DMEA), 3-dimethylamino-1-propanol (3DMA1P), 1DMA2P, diethylethanolamine (DEEA), 1DEA2P, DEAB, 1-(2-hydroxyethyl)-piperidine (1-(2HE)-PP), 1-(2-hydroxyethyl)-pyrrolidine 1-(2HE)-PRLD and triethylamine (TREA) [25, 30, 31, 49-59].

The reaction rate of tertiary amines is much lower than that of the primary and secondary amines, thus tertiary amine is normally applied as a bicarbonate forming absorbent to blend with activators. Due to strong steric hindrance, there exists an apparent reduction of second order rate constant k_2 of AMP in comparison with MEA and MAE which, however, also limits its general performance. On the other hand, the slight change from the MEA to the MAE molecule has little influence on the second order reaction rate constant. As shown in the CO_2 absorption experiment, the apparent CO_2 absorption rate of MAE solution is similar to that of MEA solution.

To conclude, MAE appears to be a competitive absorbent for CO_2

absorption/desorption. It should be pointed out that carcinogenic *N*-nitrosamines and *N*-nitramines by-products of amine degradation, may form either from secondary/tertiary amines or from the degradation products of primary amine [60]. Further research to address the degradation issue related to potentially harmful degradation products should be carefully executed to control their emission to and deposit in the surrounding environment.

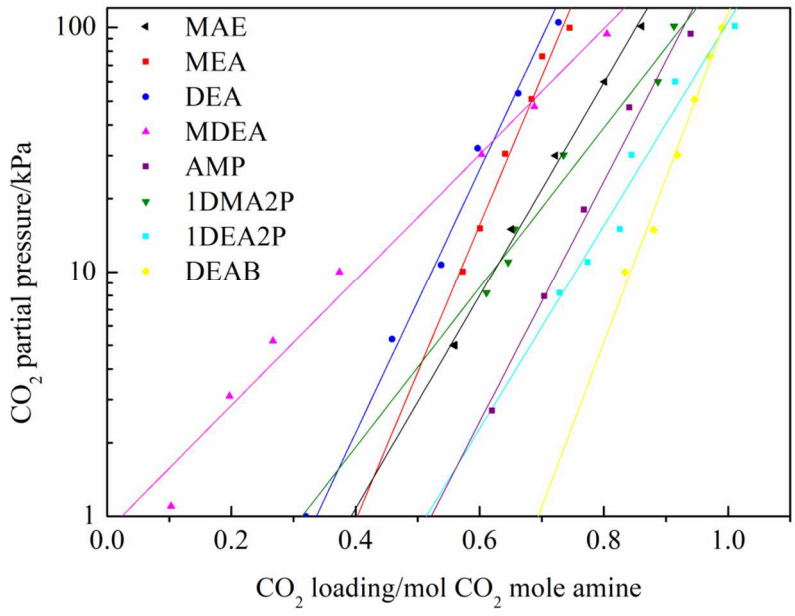

Figure 12. Equilibrium CO_2 solubility of 2 mol·L^{-1} amine solution at 313 K where points are experimental data and curves are fitting results.

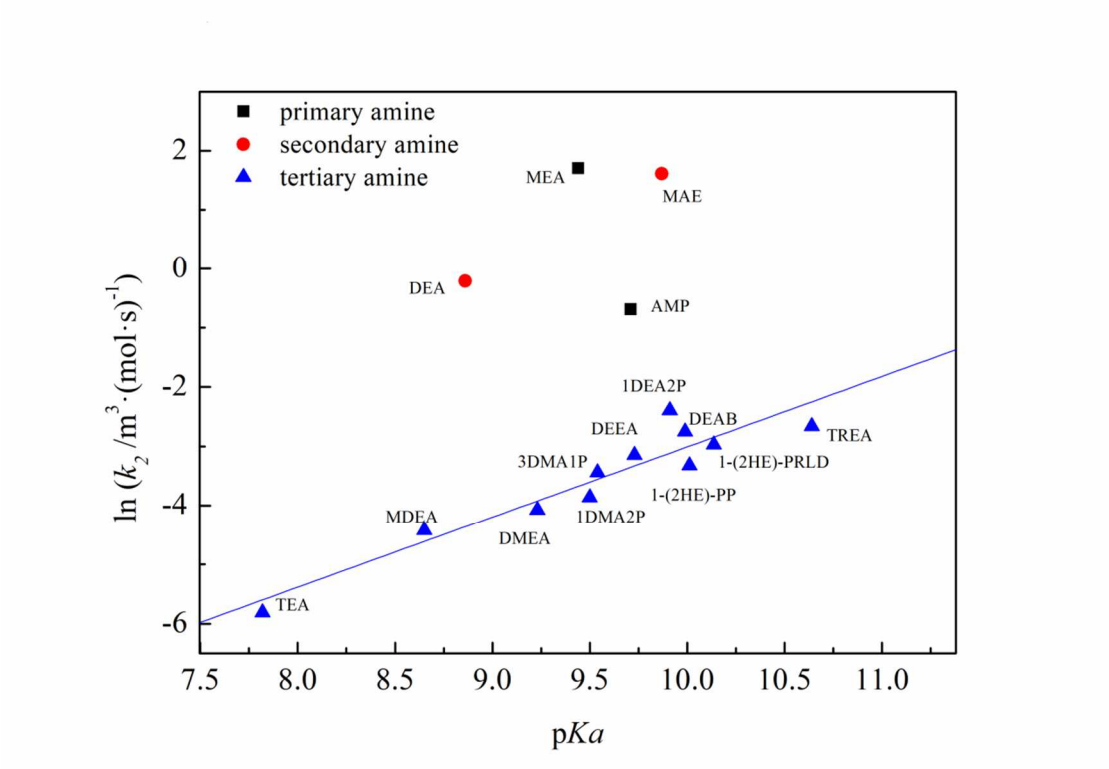

Figure 13. Second order rate constant versus p*Ka* at 298 K.

5. Conclusions

This work involves chemical reactions and phase behavior of CO_2 absorption in *N*-methylaminoethanol solution. Thermodynamic analysis connecting two different scales was carried out to study the CO_2 absorption mechanism. The dissociation and carbamate formation constants for the critical reactions involving CO_2 absorption in *N*-methylaminoethanol solution were obtained as a function of temperature. The enthalpies and entropies of the corresponding reactions were derived using the van 't Hoff equation. A thermodynamic model was developed for the *N*-methylaminoethanol -CO_2-H_2O ternary system. The predictive equilibrium CO_2 solubility agreed well with experimental data with average deviation of 4.2 %. The influence mechanism of experimental conditions such as temperature, CO_2 partial pressure was investigated.

And the prediction was successfully extrapolated outside the range of experimental conditions. Moreover, the species profiles and absorption/desorption heat for CO_2 absorption in *N*-methylaminoethanol solution were predicted using the thermodynamic model to further explore the CO_2 absorption mechanism. *N*-methylaminoethanol solution had a relatively lower regeneration energy cost in comparison with benchmark monoethanolamine solution, which is due to the impact of less stable carbamate formation.

The lab scale experiment showed that *N*-methylaminoethanol solution had higher CO_2 absorption efficiency than monoethanolamine and methyldiethanolamine solution. Based on the comprehensive evaluation of *N*-methylaminoethanol solution as a potential CO_2 absorbent for PCC, it has superior CO_2 capture performance such as fast reaction rate, high equilibrium CO_2 solubility and most importantly, low regeneration energy penalty. The unique properties of *N*-methylaminoethanol are originated from the typical secondary amine molecular structure and relative unstable carbamte formation, offering more flexibility for amine based CO_2 absorbents. However, the degradation behavior of the amine under long term operation and complex flue gas with oxidants such as O_2, SO_X and O_X should be carefully studied and controlled to further advance the popularization of PCC technology.

Acknowledgment:

Financial support from the National Natural Science Foundation of China (NSFC-Nos. 21536003, 21706057, 21776065, 21606078, 21476064 and 51521006),

the National Key Technology R&D Program (MOST-No. 2014BAC18B04), the China Outstanding Engineer Training Plan for Students of Chemical Engineering & Technology in Hunan University (MOE-No.2011-40), the Opening Project of Guangxi Colleges and Universities Key Laboratory of Beibu Gulf Oil and Natural Gas Resource Effective Utilization (2016KLOG17, 2016KLOG13, 2016KLOG11 and 2016KLOG05), the China Scholarship Council (201706130044) are gratefully acknowledged.

References

[1] MacDowell N, Florin N, Buchard A, Hallett J, Galindo A, Jackson G, et al. An overview of CO_2 capture technologies. Energ Environ Sci. 2010;3:1645-69.

[2] Wang M, Joel AS, Ramshaw C, Eimer D, Musa NM. Process intensification for post-combustion CO_2 capture with chemical absorption: A critical review. Applied Energy. 2015;158:275-91.

[3] Wu X, Wang M, Liao P, Shen J, Li Y. Solvent-based post-combustion CO_2 capture for power plants: A critical review and perspective on dynamic modelling, system identification, process control and flexible operation. Applied Energy. 2020;257:113941.

[4] Yang Q, Puxty G, James S, Bown M, Feron P, Conway W. Toward Intelligent CO_2 Capture Solvent Design through Experimental Solvent Development and Amine Synthesis. Energy & Fuels. 2016;30:7503-10.

[5] Zhang X, Zhang R, Liu H, Gao H, Liang Z. Evaluating CO_2 desorption performance in CO_2-loaded aqueous tri-solvent blend amines with and without solid acid catalysts. Applied Energy. 2018;218:417-29.

[6] Gao H, Wang N, Du J, Luo X, Liang Z. Comparative kinetics of carbon dioxide (CO_2) absorption into EAE, 1DMA2P and their blends in aqueous solution using the stopped-flow technique. International Journal of Greenhouse Gas Control. 2020;94:102948.

[7] Zhang R, Zhang X, Yang Q, Yu H, Liang Z, Luo X. Analysis of the reduction of energy cost by using MEA-MDEA-PZ solvent for post-combustion carbon dioxide capture (PCC). Applied Energy. 2017;205:1002-11.

[8] Liu S, Ling H, Lv J, Gao H, Na Y, Liang Z. New Insights and Assessment of Primary Alkanolamine/Sulfolane Biphasic Solutions for Post-combustion CO_2 Capture: Absorption, Desorption, Phase Separation, and Technological Process. Industrial & Engineering Chemistry Research. 2019;58:20461-71.

[9] Shen Y, Chen H, Wang J, Zhang S, Jiang C, Ye J, et al. Two-stage interaction performance of CO_2 absorption into biphasic solvents: Mechanism analysis, quantum calculation and energy consumption. Applied Energy. 2020;260:114343.

[10] Wanderley RR, Pinto DDD, Knuutila HK. Investigating opportunities for water-lean solvents in CO_2

capture: VLE and heat of absorption in water-lean solvents containing MEA. Separation and Purification Technology. 2020;231:115883.
[11] Puxty G, Rowland R, Allport A, Yang Q, Bown M, Burns R, et al. Carbon Dioxide Postcombustion Capture: A Novel Screening Study of the Carbon Dioxide Absorption Performance of 76 Amines. Environmental Science & Technology. 2009;43:6427-33.
[12] Hadri NE, Quang DV, Goetheer ELV, Zahra MRMA. Aqueous amine solution characterization for post-combustion CO_2 capture process. Applied Energy. 2017;185:1433-49.
[13] Kumar G, Kundu M. Vapour-liquid equilibrium of CO_2 in aqueous solutions of N-methyl-2-ethanolamine. Can J Chem Eng. 2012;90:627-30.
[14] Folgueira I, Teijido I, Garcia-Abuin A, Gomez-Diaz D, Rumbo A. 2-(Methylamino)ethanol for CO_2 Absorption in a Bubble Reactor. Energy & Fuels. 2014;28:4737-45.
[15] Mimura T, Suda T, Iwaki I, Honda A, Kumazawa H. Kinetics of Reaction Between Carbon Dioxide and Sterically Hindered Amines for Carbon Dioxide Recovery from Power Plant Flue Gases. Chem Eng Commun. 1998;170:245-160.
[16] Luo X, Su L, Gao H, Wu X, Idem RO, Tontiwachwuthikul P, et al. Density, Viscosity, and N_2O Solubility of Aqueous 2-(Methylamino)ethanol Solution. J Chem Eng Data. 2016;62:129-40.
[17] Kent RL, Eisenberg B. Better data for amine treating. Hydrocarbon Processing. 1976;55:87-90.
[18] Deshmukh RD, Mather AE. A mathematical model for equilibrium solubility of hydrogen sulfide and carbon dioxide in aqueous alkanolamine solutions. Chem Eng Sci. 1981;36:355-62.
[19] Benamor A, Aroua MK. Modeling of CO_2 solubility and carbamate concentration in DEA, MDEA and their mixtures using the Deshmukh-Mather model. Fluid Phase Equilibria. 2005;231:150-62.
[20] Goharrokhi M, Taghikhani V, Ghotbi C, Safekordi AA. Correlation and Prediction of Solubility of CO_2 in Amine Aqueous Solutions. Iran J Chem Chem Eng. 2010;29:111-24.
[21] Afkhamipour M, Mofarahi M. Experimental measurement and modeling study on CO_2 equilibrium solubility, density and viscosity for 1-dimethylamino-2-propanol (1DMA2P) solution. Fluid Phase Equilibria. 2018;457:38-51.
[22] Pakzad P, Mofarahi M, Izadpanah AA, Afkhamipour M, Lee C-H. An experimental and modeling study of CO_2 solubility in a 2-amino-2-methyl-1-propanol (AMP) + N-methyl-2-pyrrolidone (NMP) solution. Chem Eng Sci. 2018;175:365-76.
[23] Aroua MK, Amor AB, Haji-Sulaiman MZ. Temperature Dependency of the Equilibrium Constant for the Formation of Carbamate From Diethanolamine. J Chem Eng Data. 1997;42:692-6.
[24] Xiao M, Liu H, Idem R, Tontiwachwuthikul P, Liang Z. A study of structure-activity relationships of commercial tertiary amines for post-combustion CO_2 capture. Applied Energy. 2016;184:219-29.
[25] Littel RJ, Bos M, Knoop GJ. Dissociation Constants of Some Alkanolamines at 293, 303, 318, and 333 K. J Chem Eng Data. 1990;35:276-7.
[26] Edwards TJ, Maurer G, Newman J. Vapor-liquid equilibria in multicomponent aqueous solutions of volatile weak electrolytes. AIChE Journal. 1978;24:966-76.
[27] Chen C-C, Britt HI, Boston JF, Evans LB. Extension and application of the pitzer equation for vapor-liquid equilibrium of aqueous electrolyte systems with molecular solutes. AIChE Journal. 1979;25:820-31.
[28] Aroua MK, Benamor A, Haji-Sulaiman MZ. Equilibrium Constant for Carbamate Formation from Monoethanolamine and Its Relationship with Temperature. J Chem Eng Data. 1999;44:887-91.
[29] Perrin DD. Dissociation constants of Organic Bases in Aqueous Solution. Butterworths: London. 1965.

[30] Rayer AV, Sumon KZ, Jaffari L, Henni A. Dissociation Constants (p*Ka*) of Tertiary and Cyclic Amines: Structural and Temperature Dependences. J Chem Eng Data. 2014;59:3805.
[31] Fernandes D, Conway W, Wang X, Burns R, Lawrance G, Maeder M, et al. Protonation constants and thermodynamic properties of amines for post combustion capture of CO_2. J Chem Thermodynamics. 2012;51:97-102.
[32] Peng D-Y, Robinson DB. A New Two-Constant Equation of State. Ind Eng Chem Fundamen. 1976;15:59-64.
[33] Haider HAM, Yusoff R, Aroua MK. Equilibrium solubility of carbon dioxide in 2(methylamino)ethanol. Fluid Phase Equilibria. 2011;303:162-7.
[34] Kumar G. Vapour-liquid Equilibrium of Carbon Dioxide in Newly Proposed Blends of Alkanolamines. Pd D Thesis, NIT Rourkela. 2013.
[35] Li K, Yu H, Feron P, Tade M, Wardhaugh L. Technical and Energy Performance of an Advanced, Aqueous Ammonia-Based CO_2 Capture Technology for a 500 MW Coal-Fired Power Station. Environmental Science & Technology. 2015;49:10243-52.
[36] Feng B, Du M, Dennis TJ, Anthony K, Perumal MJ. Reduction of Energy Requirement of CO_2 Desorption by Adding Acid into CO_2-Loaded Solvent. Energy & Fuels. 2010;24:213-9.
[37] Zhang S, Lu Y. Surfactants Facilitating Carbonic Anhydrase Enzyme-Mediated CO_2 Absorption into a Carbonate Solution. Environmental Science & Technology. 2017;51:8537-43.
[38] Li K, Leigh W, Feron P, Yu H, Tade M. Systematic study of aqueous monoethanolamine (MEA)-based CO_2 capture process: Techo-economic assessment of the MEA process and its improvements. Applied Energy. 2016;165:648-59.
[39] Oyenekan BA, Rochelle GT. Alternative stripper configurations for CO_2 capture by aqueous amines. AIChE Journal. 2007;53:3144-54.
[40] Svendsen HF, Hessen ET, Mejdell T. Carbon dioxide capture by absorption, challenges and possibilities. Chemical Engineering Journal. 2011;171:718-24.
[41] Kim I, Hoff KA, Hessen ET, Haug-Warberg T, Svendsen HF. Enthalpy of absorption of CO_2 with alkanolamine solutions predicted from reaction equilibrium constants. Chem Eng Sci. 2009;64:2027-38.
[42] Kim I, Svendsen HF. Heat of Absorption of Carbon Dioxide (CO_2) in Monoethanolamine (MEA) and 2-(Aminoethyl)ethanolamine (AEEA) Solutions. Ind Eng Chem Res. 2007;46:5803-9.
[43] Jou F-Y, Otto FD, Mather AE. Vapor-Liquid Equilibrium of Carbon Dioxide in Aqueous Mixtures of Monoethanolamine and Methyldiethanolamine. Ind Eng Chem Res. 1994;33:2002-5.
[44] Xiao M, Liu H, Gao H, Liang Z. CO_2 absorption with aqueous tertiary amine solutions: Equilibrium solubility and thermodynamic modeling. The Journal of Chemical Thermodynamics. 2018;122:170-82.
[45] Maneeintr K, Idem RO, Tontiwachwuthikul P, Wee AGH. Synthesis, Solubilities, and Cyclic Capacities of Amino Alcohols for CO_2 Capture from Flue Gas Streams. Energy Procedia. 2009;1:1327-34.
[46] Liang Y, Liu H, Rongwong W, Liang Z, Idem R, Tontiwachwuthikul P. Solubility, absorption heat and mass transfer studies of CO_2 absorption into aqueous solution of 1-dimethylamino-2-propanol. Fuel. 2015;144:121-9.
[47] Liu H, Xiao M, Liang Z, Tontiwachwuthikul P. The Analysis of Solubility, Absorption Kinetics of CO_2 Absorption into Aqueous 1-Diethylamino-2-Propanol Solution. AIChE Journal. 2017;63:2694-704.
[48] Tontiwachwuthikul P, Meisen A, Lim CJ. Solubility of CO_2 in 2-Amino-2-mehtyl-1-propanol Solutions. J Chem Eng Data. 1991;36:130-3.

[49] Ali SH, Merchant SQ, Fahim MA. Reaction kinetics of some secondary alkanolamines with carbon dioxide in aqueous solutions by stopped flow technique. Sep Puri Tech. 2002;27:121-36.
[50] Liu H, Xiao M, Liang Z, Rongwong W, Li J, Tontiwachwuthikul P. Analysis of Reaction Kinetics of CO_2 Absorption into a Novel 1-(2-Hydroxyethyl)-piperidine Solvent Using Stopped-Flow Technique. Ind Eng Chem Res. 2015;54:12525-33.
[51] Liu H, Liang Z, Sema T, Rongwong W, Li C, Na Y, et al. Kinetics of CO_2 Absorption into a Novel 1-Diethylamino-2-propanol Solvent Using Stopped-Flow Technique. AIChE Journal. 2014;60:3502-10.
[52] Liu H, Li M, Idem R, Tontiwachwuthikul P, Liang Z. Analysis of solubility, absorption heat and kinetics of CO_2 absorption into 1-(2-hydroxyethyl)pyrrolidine solvent. Chem Eng Sci. 2017;162:120-30.
[53] Kadiwala S, Rayer AV, Henni A. Kinetics of carbon dioxide (CO_2) with ethylenediamine, 3-amino-1-propanol in methanol and ethanol, and with 1-dimethylamino-2-propanol and 3-dimethylamino-1-propanol in water using stopped-flow technique. Chem Eng J. 2012;179:262-71.
[54] Liu H, Sema T, Liang Z, Fu K, Idem R, Na Y, et al. CO_2 absorption kinetics of 4-diethylamino-2-butanol solvent using stopped-flow technique. Sep Puri Tech. 2014;136:81-7.
[55] Versteeg GF, Dijck LAJV, Swaaij WPMV. On the kinetics between CO_2 and alkanolamines both in aqueous and non-aqueous solutions. An overview. Chem Eng Commun. 1996;144:113-58.
[56] Ali SH. Kinetics of the Reaction of Carbon Dioxide with Blends of Amines in Aqueous Media Using the Stopped-Flow Technique. Int J Chem Kinet. 2005;2005:7.
[57] Li J, Henni A, Tontiwachwuthikul P. Reaction Kinetics of CO_2 in Aqueous Ethylenediamine, Ethyl Ethanolamine, and Diethyl Monoethanolamine Solutions in the Temperature Range of 298-313 K, Using the Stopped-Flow Technique. ind Eng Chem Res. 2007;46:4426-34.
[58] Littel RJ, Swaaij WPMV, Versteeg GF. Kinetics of Carbon Dioxide with Tertiary Amines in aqueous solution. AIChE Journal. 1990;36:1633-40.
[59] Alper E. Reaction Mechanism and Kinetics of Aqueous Solutions of 2-Amino-2-methyl-1-propanol and Carbon Dioxide. Ind Eng Chem Res. 1990;29:1725-8.
[60] Chen X, Huang G, An C, Yao Y, Zhao S. Emerging *N*-nitrosamines and *N*-nitramines from amine-based post-combustion CO_2 capture - A review. Chem Eng J. 2018;335:921-35.